Pis'ma v ZhETF, vol. 100, iss. 5, pp. 374 – 378

On the superconductivity of graphite interfaces

P. Esquinazi[1)], *T. T. Heikkilä*[+], *Y. V. Lysogorskiy*[*], *D. A. Tayurskii*[*×], *G. E. Volovik*[°▽]

Division of Superconductivity and Magnetism, Institut für Experimentelle Physik II, Universität Leipzig, D-0413 Leipzig, Germany

[+]*Department of Physics and Nanoscience Center, University of Jyväskylä, FI-40014 Jyväskylä, Finland*

[*]*Institute of Physics, Kazan Federal University, 420008 Kazan, Russia*

[×]*Centre for Quantum Technologies, Kazan Federal University, 420008 Kazan, Russia*

[°]*Low Temperature Laboratory, Aalto University, FI-00076 Aalto, Finland*

[▽]*Landau Institute for Theoretical Physics of the RAS, 142432 Chernogolovka, Russia*

Submitted 24 July 2014

We propose an explanation for the appearance of superconductivity at the interfaces of graphite with Bernal stacking order. A network of line defects with flat bands appears at the interfaces between two slightly twisted graphite structures. Due to the flat band the probability to find high temperature superconductivity at these quasi one-dimensional corridors is strongly enhanced. When the network of superconducting lines is dense it becomes effectively two-dimensional. The model provides an explanation for several reports on the observation of superconductivity up to room temperature in different oriented graphite samples, graphite powders as well as graphite-composite samples published in the past.

DOI: 10.7868/S0370274X14170093

Highly oriented pyrolytic graphite (HOPG) is known to have quasi two-dimensional (2D) interfaces [1, 2]. Recently, it was found that such interfaces exhibit extraordinary properties that indicate the existence of granular 2D superconductivity within the interfaces and up to the room temperature or above [3–5]. Here we discuss a possible origin of this phenomenon.

The interface in graphite we discuss in this work represents a grain boundary between domains with slightly different orientations and can be recognised by transmission electron microscopy with the electron beam applied parallel to the graphene planes of graphite. Fig. 1 shows transmission electron microscopy pictures of two HOPG samples at different resolutions. The interfaces are at the borders of the crystalline (Bernal stacking order ABA...) regions characterised by a certain gray colour. The twist angle $\theta_{\rm twist}$, i.e., a rotation with respect to the c-axis between single crystalline domains of Bernal graphite, may vary from $\sim 1^\circ$ to $< 60^\circ$ [7], while the tilting angle of the grains with respect to the c-axis $\theta_c \lesssim 0.4^\circ$ for the highest oriented pyrolytic graphite samples. When the misfit angle is small enough, the grain boundary can be represented by a system of dislocations – the Burgers–Bragg–Read–Shockley (BBRS) dislocation model [8–10]. This is the system of edge dislocations if $\theta_c \neq 0$, and the system of screw dislocations in the case $\theta_{\rm twist} \neq 0$.

The BBRS dislocation model of the interface between two domains with slightly different orientations – a small twist angle $\theta_{\rm twist}$ – is demonstrated in Fig. 2. For simplicity the interface is illustrated using two twisted sheets forming square lattices. In Fig. 2 (left) is the initial configuration, when two domains are stuck together; in Fig. 2 (right) is the relaxed configuration of the interface. The latter consists of perfectly matched regions separated by the network of the linear objects – solitons in the case of two sheets and screw dislocations in the case of real interface. The size L of the perfect regions is determined by $\theta_{\rm twist}$ in the equation $L \sim a/\sin(\theta_{\rm twist}/2)$, where a is the interatomic distance [10]. For bilayer graphene with slightly twisted layers, the solitons and their networks can be found in Refs. [11–13].

The network of linear defects is formed when the twist angle is small enough. For bilayer graphene the defects emerge when $\theta_{\rm twist} \lesssim 1^\circ$ [12]. For larger angles the configuration of the type of Fig. 2 (left) is preferable, in which the twist angle between the layers does not change. This configuration gives rise to Moiré pat-

[1)]e-mail: esquin@physik.uni-leipzig.de

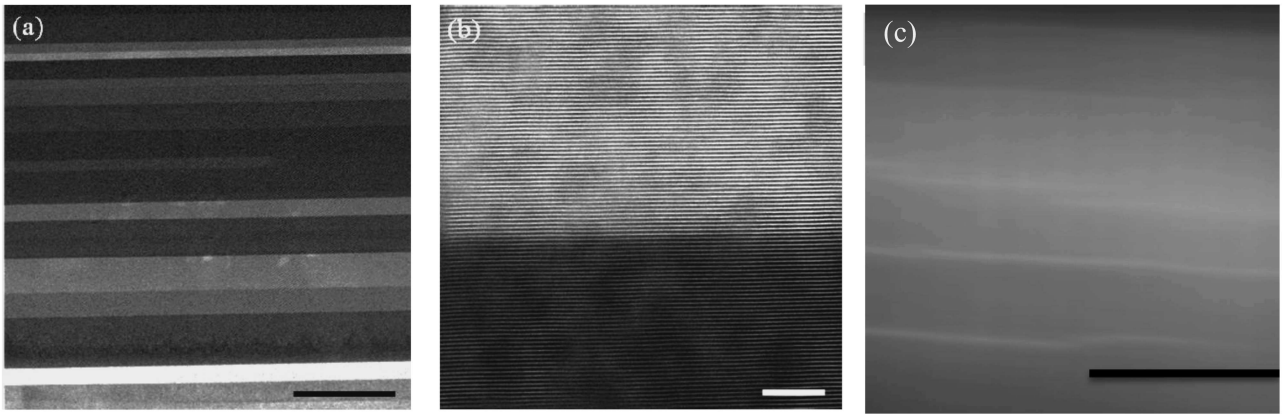

Fig. 1. (a) – Transmission electron microscope picture of a HOPG lamella of grade A. The scale bar corresponds to 500 nm. The graphene planes run parallel to the interfaces. (b) – A zoom of a section of (a) with higher resolution where the edges of the graphene planes can be recognized. The c-axis is normal to the graphene planes. The scale bar corresponds to 5 nm [6]. (c) – Similar but for a HOPG sample of grade B and from a different source. The bar corresponds to 1 μm. In this sample there is less area with well defined interfaces than in grade A samples

terns as has been reported in the literature recently, see, e.g., [7, 14–17].

Graphite represents the ordered or disordered array of the two-dimensional graphene sheets. Graphene is the topological material, which belongs to the class of topological semimetals [18]. Its electronic energy spectrum has topologically protected point nodes [19]. In graphite, the point nodes in each layer transform to the chain of the electron and hole Fermi surfaces [20], which corresponds to approximate line of zeroes protected by topology. That is why graphite experiences (at least approximately) the properties, which are generic for the topological matter [21, 22].

In the topological materials, the topological defects such as dislocations, quantized vortices, domain walls, solitons, grain boundaries, etc., frequently contain exotic gapless branches in the electronic spectrum. In particular, the networks of solitons in the twisted bilayer graphene contains topologically protected helical modes, which is the direct consequence of the twist [12]. For us it is important that among the gapless branches there are Dirac points with quadratic and higher order touching of branches, and the completely dispersionless branch with zero energy – the flat band. The topologically protected flat band arises at the zig-zag edge of a graphene sheet [23]; inside Abrikosov vortex in Weyl superconductor [24–26]; at the grain boundary in graphene, which is represented by the chain of the point edge dislocations [27]. In graphite, which is only approximately a topological material, the flat bands are also approximate. Such flat band arises on the surface or at the interface of the rhombohedral graphite [28], where it actually represents the Dirac point with quadratic spectrum and with extremely large mass [29].

The situation, which is similar to the interfaces in the Bernal graphite, is discussed for IV–VI semiconductor heterostructures consisting of a topological crystalline insulator and a trivial insulator [30]. Due to the lattice mismatch between insulators, the two-dimensional square array of dislocations with period of 3–25 nm is spontaneously formed at the interface, which leads to a nearly flat band there. The topological origin of this flat band can be understood in terms of the pseudo-magnetic field created by strain and the corresponding Landau levels. Note that a similar pseudo-magnetic field emerges in the strained graphene [31]. All this suggests that in a similar manner the network of screw dislocations at the graphite interface may also lead to exotic branches with almost the flat spectrum. This is supported by consideration of the edge dislocations in graphite. They can be represented as the edges of the extra layers of the graphene sheets, which as we know contain flat bands.

The important consequence of the flattening of the electronic spectrum is the singular density of states $N(\epsilon)$ at $\epsilon \to 0$. This produces ferromagnetism, superconductivity or another ordered state, with high transition temperature. In particular, in the presence of the flat band one has $N(\epsilon) \propto \delta(\epsilon)$ and one obtains the linear dependence $T_c \propto g$ of the critical temperature on the interaction strength in the Cooper channel [32, 28, 29, 33]. The quadratic flattening in 1D systems gives $N(\epsilon) \propto \epsilon^{-1/2}$ and the quadratic dependence $T_c \propto g^2$ of the critical temperature [34, 35]. This is in clear contrast to the

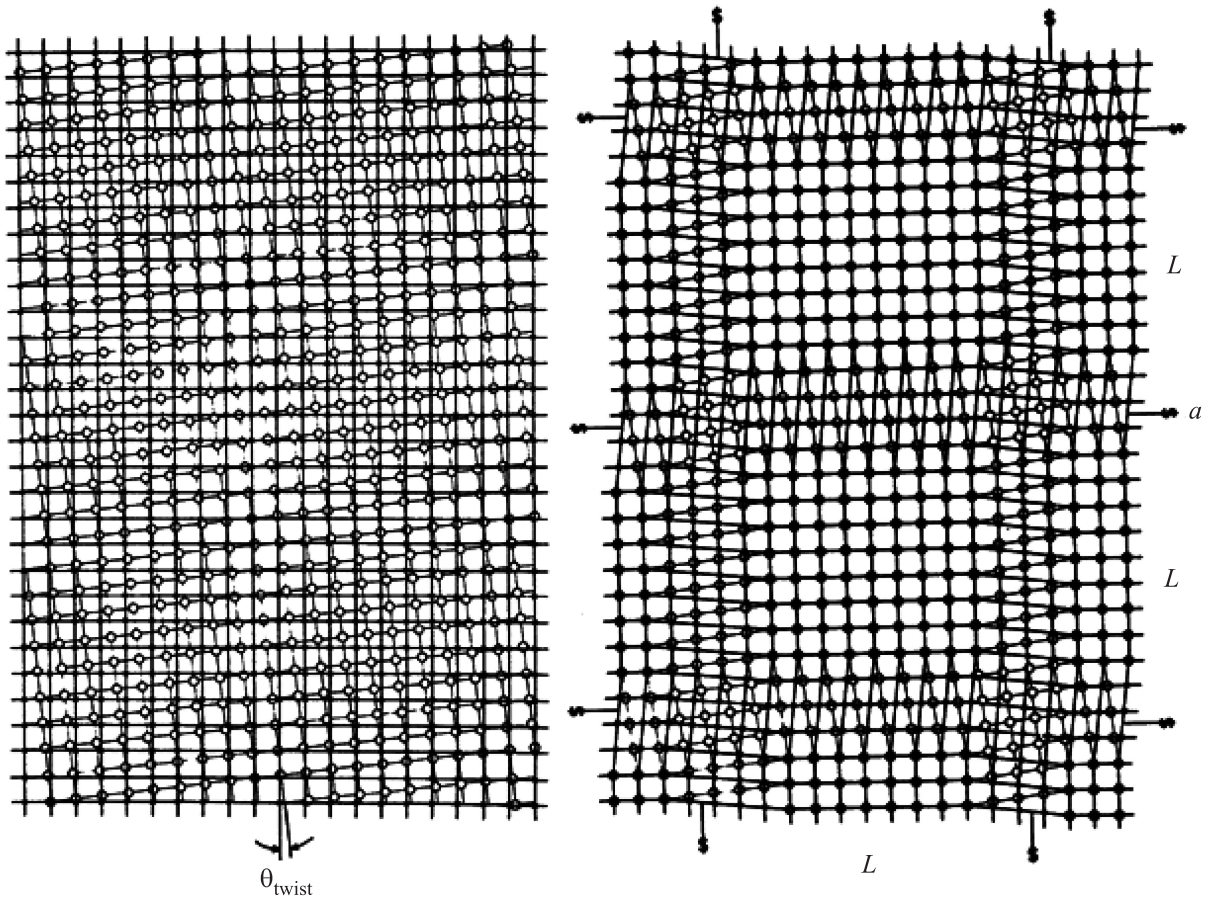

Fig. 2. The illustration of the dislocation model of the crystal grain boundary [10] in the case of the interface between two domains with slightly different orientations – a small twist angle $\theta_{\rm twist}$. On the left is the initial configuration, when two domains are stuck together; on the right is the relaxed configuration of the interface. The latter consists of perfectly matched regions of size $L \sim a/\sin(\theta_{\rm twist}/2)$ separated by the network of linear objects – the screw dislocations. For simplicity the interface is illustrated using two twisted sheets of quadratic lattice. Here instead of dislocations, the twist between the layers is mediated by solitons – boundaries between the matched regions

exponential behavior, $T_c \propto \exp(-1/g)$, in conventional superconductivity. As pointed out in Ref. [30], in the IV–VI semiconductor multilayers the transition temperature is unusually high for these materials, while the strong anisotropy of the upper critical field reveals the two-dimensional character of superconductivity. The authors of Ref. [30] ascribe that to the flat band emerging from the misfit dislocation array at the interface between topological and non-topological insulators. This proposal coordinates and with experiments on highly oriented pyrolytic graphite, where the unusually high transition temperature is reported, which is associated with the graphite interfaces [5, 3].

In the highly oriented graphite the dislocation network at the interface is dense, with $L \sim 10\,$nm. That is why the superconducting state, if it is formed in the 1D "corridors", has effectively a two-dimensional nature with possible flux quantization. We note that a misfit in the c-axis orientation may also lead to a similar result, because it would give rise to an array of straight edge dislocations, each containing a 1D flat band.

There is another, non-topological, source of the flattening of the electronic spectrum: it is the effect of electron-electron interaction [32, 36]. In particular, this mechanism is operating in the vicinity of the van Hove singularity [25, 37]. Note, that experimental STM and STS studies in bilayer [15, 16] as well as in multilayer graphene [7, 17] demonstrated the existence of logarithmic van Hove singularities for $1^\circ \lesssim \theta_{\rm twist} \lesssim 10^\circ$. The van Hove singularity appears on the "light" (from STM picture) domains of twisted bilayer, which corresponds to the Moiré pattern.

The model of the interface superconductivity, which we propose, may account for several details of differ-

ent publications reporting superconducting-like signals up to room temperature in graphite-based as well as annealed carbon samples in the last 40 years [38–45]. In particular one can understand why those signals were difficult to reproduce, not always stable in time, relatively weak, i.e. appeared to come from a small amount of superconducting mass, and very sensitive to the preparation conditions. According to Ref. [12], the topological protection of the fermion zero modes leaving in the 1D corridors is weak, and can be broken by atomic vacancies or small adsorbates. That is why future theoretical work should study the influence of doping (through hydrogen, for example) at the interfaces. Local transport measurements of single interfaces in multilayer graphene samples with different twist angles are of interest.

The ideas drawn in this letter are the result of the discussions at the Workshop on flat bands and room-temperature superconductivity, held in Otaniemi, Finland, May 30–31. P.E. acknowledges discussions with R.G. Mints during his stay at Tel-Aviv University, Ana Ballestar for providing the pictures of her thesis and Dr. Pipple and Dr. Böhlmann for the TEM measurements. G.E.V. and T.T.H. acknowledges the financial support by the Academy of Finland through its LTQ CoE grant (project # 250280). Y.V.L. and D.A.T. acknowledge the Russian Government Program of Competitive Growth of Kazan Federal University.

1. M. Inagaki, *New Carbons: Control of Structure and Functions*, Elsevier (2000).
2. J. Barzola-Quiquia, J.-L. Yao, P. Rödiger, K. Schindler, and P. Esquinazi, Phys. Stat. Sol. (a) **205**, 2924 (2008).
3. A. Ballestar, J. Barzola-Quiquia, T. Scheike, and P. Esquinazi, New J. Phys. **15**, 023024 (2013).
4. T. Scheike, W. Böhlmann, P. Esquinazi, J. Barzola-Quiquia, A. Ballestar, and A. Setzer, Adv. Mater. **24**, 5826 (2012).
5. T. Scheike, P. Esquinazi, A. Setzer, and W. Böhlmann, Carbon **59**, 140 (2013).
6. Taken from the Ph.D. Thesis of Ana Ballestar, entitled "Superconductivity at Graphite Interfaces" defended at the University of Leipzig (2014). The high resolution TEM pictures were taken in the "Max Planck Institute of Microstructure Physics" in Halle (Germany) by Dr. Pipple, the lower resolution TEM picture was taken by Dr. W. Böhlmann at the University of Leipzig.
7. J. H. Warner, M. H. Römmeli, T. Gemming, B. Büchner, and G. A. D. Briggs, Nano Letters **9**(1), 102 (2009).
8. J. Burgers, Proc. Phys. Soc. **52**, 23 (1940).
9. W. L. Bragg, Proc. Phys. Soc. **52**, 105 (1940).
10. W. T. Read and W. Shockley, Phys. Rev. **78**, 275 (1950).
11. J. S. Alden, A. W. Tsen, P. Y. Huang, R. Hovden, L. Brown, J. Park, D. A. Muller, and P. L. McEuen, Proc. Nat. Acad. Sci. **110**(28), 11256 (2013).
12. P. San-Jose and E. Prada, Phys. Rev. B **88**, 121408(R) (2013).
13. X. Gong and E. J. Mele, Phys. Rev. B **89**, 121415 (2014).
14. R. Bistritzer and A. MacDonald, PNAS **108**, 12233 (2011).
15. I. Brihuega, P. Mallet, H. González-Herrero, G. T. de Laissardière, M. M. Ugeda, L. Magaud, J. M. Gómez-Rodríguez, F. Ynduráin, and J.-Y. Veuillen, Phys. Rev. Lett. **109**, 196802 (2012).
16. M. Flores, E. Cisternas, J. Correa, and P. Vargas, Chem. Phys. **423**, 49 (2013).
17. L.-J. Yin, J.-B. Qiao, W.-X. Wang, Z.-D. Chu, K. F. Zhang, R.-F. Dou, C. L. Gao, J.-F. Jia, J.-C. Nie, and L. He, Phys. Rev. B **89**, 205410 (2014).
18. A. A. Burkov and L. Balents, Phys. Rev. Lett. **107**, 127205 (2011).
19. G. E. Volovik, *Springer Lecture Notes in Physics* (2007), v. 718, p. 31.
20. J. W. McClure, Phys. Rev. **108**, 612 (1957).
21. M. Z. Hasan and C. L. Kane, Rev. Mod. Phys. **82**, 3045 (2010).
22. X.-L. Qi and S.-C. Zhang, Rev. Mod. Phys. **83**, 1057 (2011).
23. S. Ryu and Y. Hatsugai, Phys. Rev. Lett. **89**, 077002 (2002).
24. Y. Kopnin and M. Salomaa, Phys. Rev. B **44**, 9667 (1991).
25. G. Volovik, JETP Lett. **59**, 830 (1994).
26. G. Volovik, JETP Lett. **70**, 609 (1999).
27. L. Feng, X. Lin, L. Meng, J.-C. Nie, J. Ni, and L. He, Appl. Phys. Lett. **101**, 113113 (2012).
28. T. Heikkilä, N. B. Kopnin, and G. Volovik, JETP Lett. **94**, 233 (2011).
29. N. B. Kopnin, M. Ijäs, A. Harju, and T. T. Heikkilä, Phys. Rev. B **87**, 140503 (2013).
30. E. Tang and L. Fu, arXiv:1403.7523 (2014).
31. F. de Juan, J. L. Mañes, and M. A. H. Vozmediano, Phys. Rev. B **87**, 165131 (2013).
32. V. Khodel and V. Shaginyan, JETP Lett. **51**, 553 (1990).
33. N. B. Kopnin, T. T. Heikkilä, and G. E. Volovik, Phys. Rev. B **83**, 220503 (2011).
34. Y. Kopaev, JETP **31**, 544 (1970).
35. Y. Kopaev and A. Rusinov, Phys. Lett. A **121**, 300 (1987).
36. A. Shashkin, V. Dolgopolov, J. Clark, V. Shaginyan, M. Zverev, and V. Khodel, arXiv:1404.7465 (2014).
37. D. Yudin, D. Hirschmeier, H. Hafermann, O. Eriksson, A. I. Lichtenstein, and M. I. Katsnelson, Phys. Rev. Lett. **112**, 070403 (2014).

38. K. Antonowicz, Nature **247**, 358 (1974).
39. Y. Kopelevich, P. Esquinazi, J. Torres, and S. Moehlecke, J. Low Temp. Phys. **119**, 691 (2000).
40. R. R. da Silva, J. H. S. Torres, and Y. Kopelevich, Phys. Rev. Lett. **87**, 147001 (2001).
41. H.-P. Yang, H.-H. Wen, Z.-W. Zhao, and S.-L. Li, Chin. Phys. Lett. **18**, 1648 (2001).
42. S. Moehlecke, P. C. Ho, and M. B. Maple, Phil. Mag. B **82**, 1335 (2002).
43. I. Felner and Y. Kopelevich, Phys. Rev. B **79**, 233409 (2009).
44. I. Felner, Materials Research Express **1**, 016001 (2014).
45. P. Esquinazi, Papers in Physics **5**, 050007 (2013).